

Supplementary Information

Low-threshold cavity-enhanced superfluorescence in polyhedral quantum dot superparticles

Xinjie Li,^{a,b} Linqi Chen,^{*a} Danqun Mao,^c Jingzhou Li,^d Wei Xie,^c Hongxing Dong^{*a,d} and Long Zhang^{*a,b,d}

^a Key Laboratory of Materials for High-Power Laser, Shanghai Institute of Optics and Fine Mechanics, Chinese Academy of Sciences, Shanghai 201800, China

^b School of Physical Science and Technology, ShanghaiTech University, Shanghai 201210, China

^c State Key Laboratory of Precision Spectroscopy, School of Physics and Electronic Science, East China Normal University, Shanghai 200241, China

^d Hangzhou Institute for Advanced Study, University of Chinese Academy of Sciences, No.1, Sub-Lane Xiangshan, Xihu District, Hangzhou 310024, China

*Corresponding author: chenlq@siom.ac.cn; hongxingd@siom.ac.cn; lzhang@siom.ac.cn.

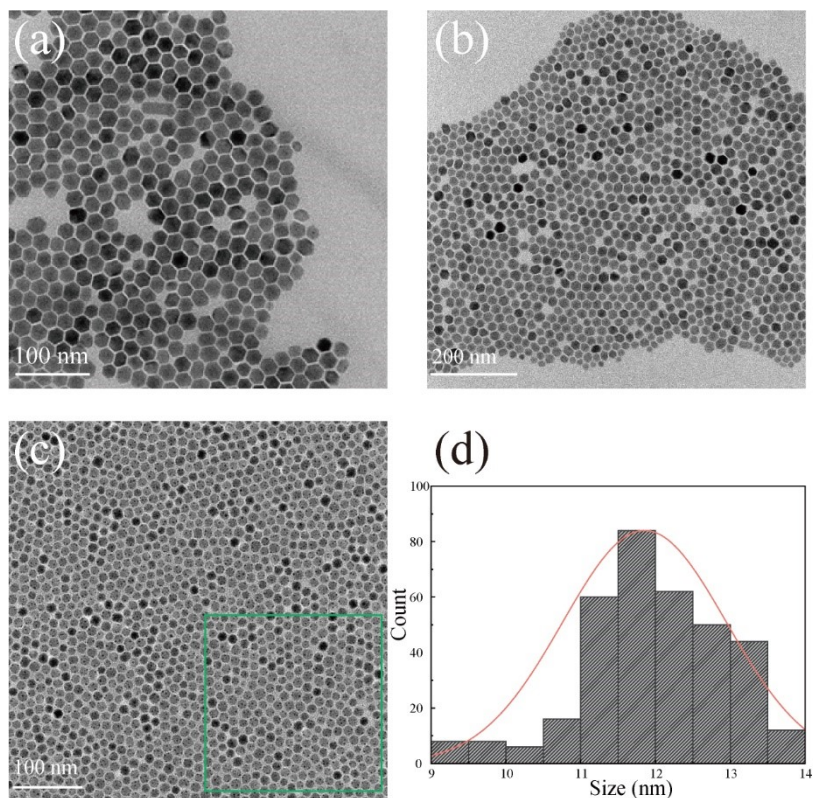


Fig. S1 Size distribution and statistics of QDs. (a-c) TEM of monodispersed 12-QDs. (d) Histogram of the size distribution of QDs in the green selections from Figure S1c. The average size is 12 nm, with deviation of ± 2 nm.

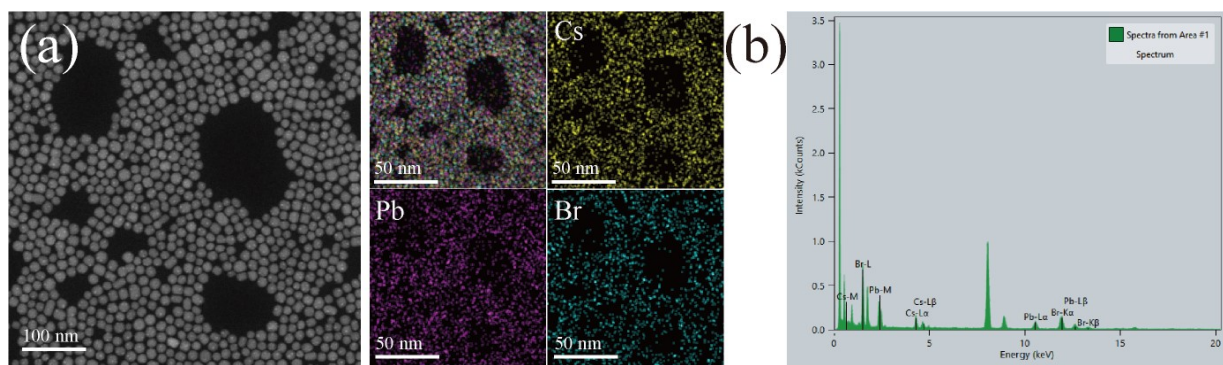


Fig. S2 The elemental composition of the 12-QDs. (a) EDS patterns. (b) Spectra spectrum.

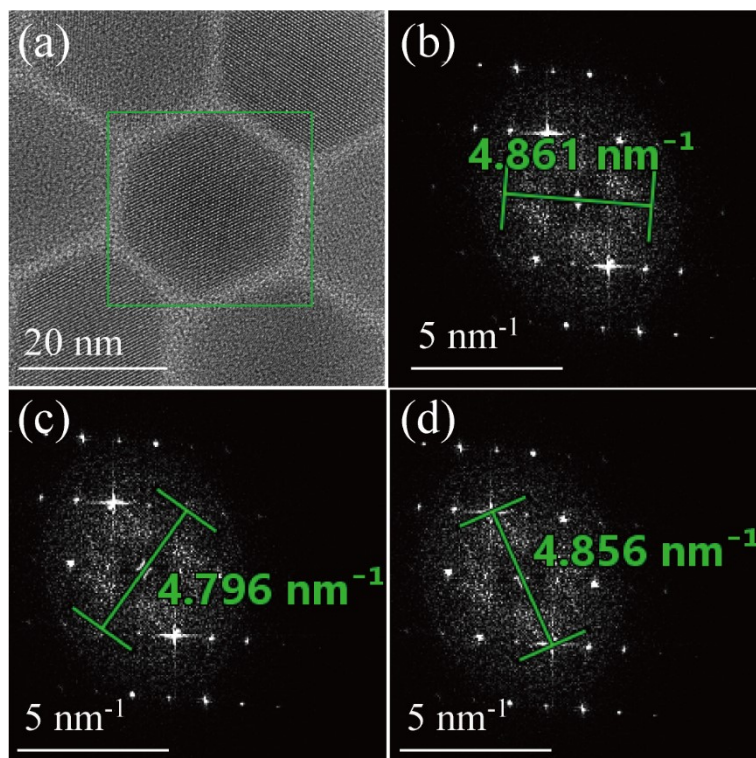


Fig. S3 (a) High-resolution TEM image of a single CsPbBr₃ 12-QDs. b-d) Corresponding FFT in the green selections.

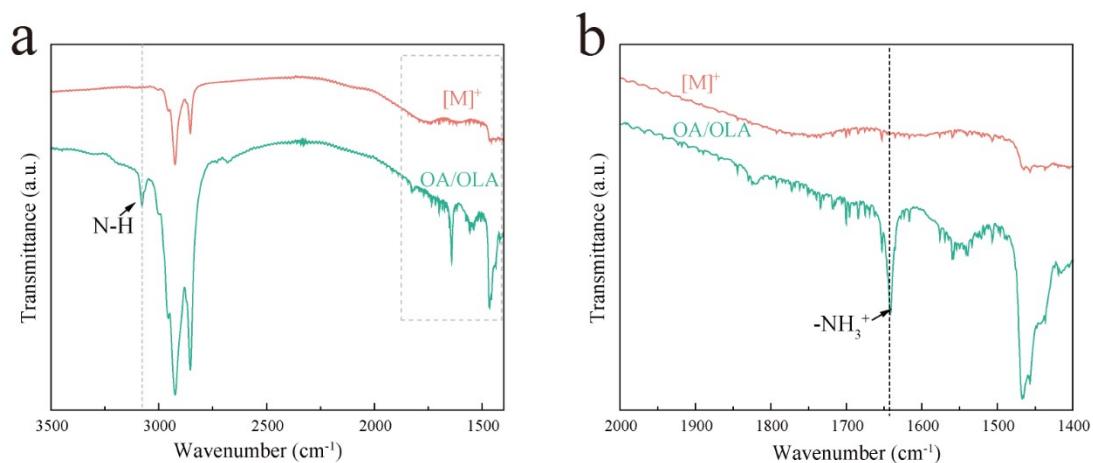


Fig. S4 FTIR spectra of 12-QDs (red) and 6-QDs (green). (a) The disappearance of the characteristic peak of the N-H stretching vibration (3100 cm^{-1}) proves the generation of tertiary ammonium ions. (b) The absence of oleylamine ligands on 12-QDs was demonstrated by the characteristic peaks of NH_3^+ (1645 cm^{-1}). $[\text{M}^+]$ represents the tertiary ammonium ions modification on 12-QDs. OA/OLA represents the oleylamine modification on 12-QDs. The disappearance of the 3100 cm^{-1} and the 1645 cm^{-1} characteristic peaks confirms the transformation of OA/OLA-capped ligands to tertiary ammonium ions.

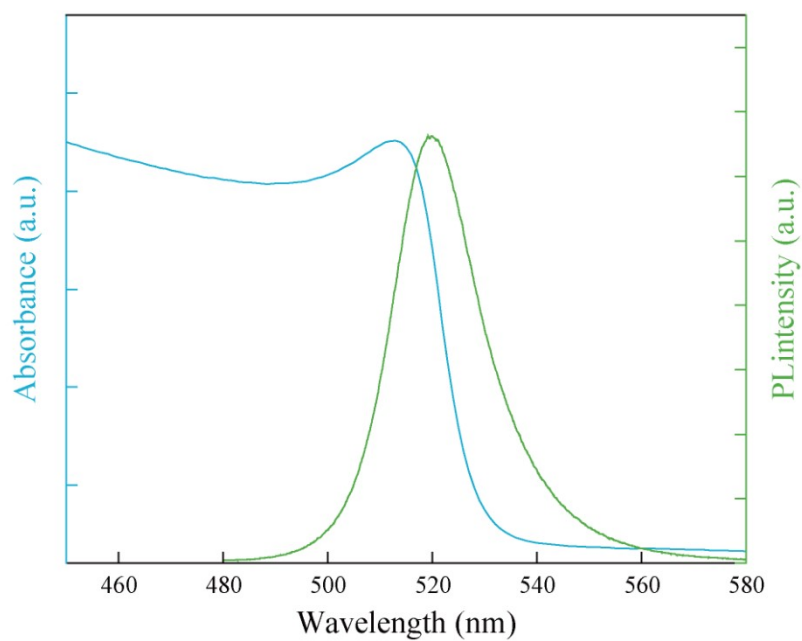


Fig. S5 UV-vis absorption and photoluminescence spectra of 12-QDs.

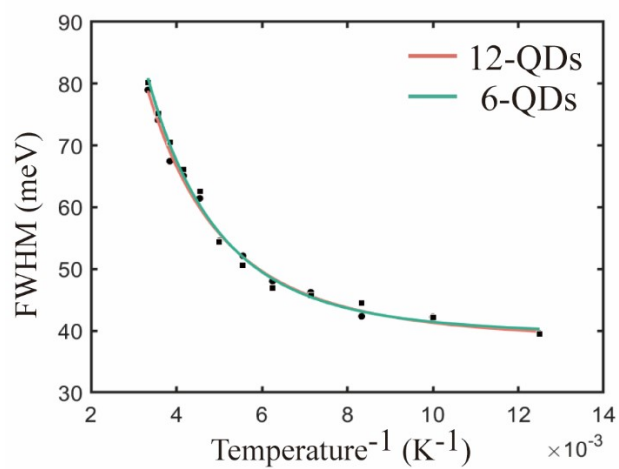


Fig. S6 Evolution of FWHM for 12-QDs and 6-QDs as temperature changes from 77K to 300K.

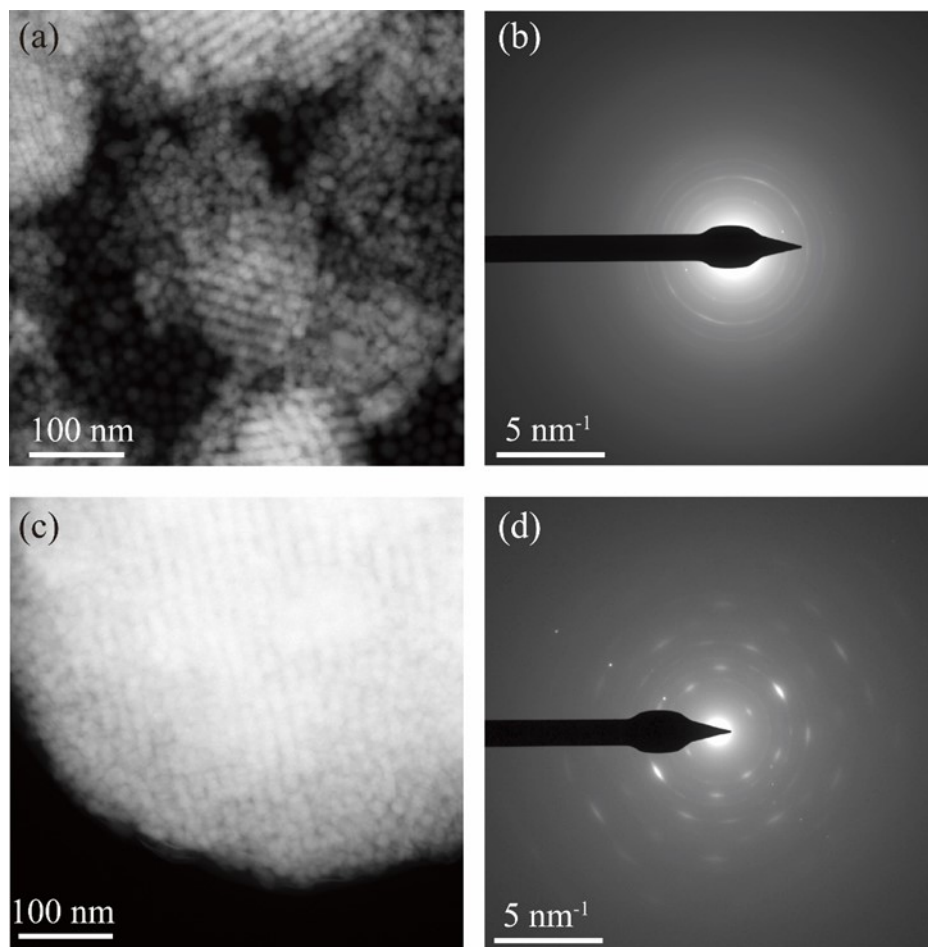


Fig. S7 (a) HAADF-TEM image of low-ordered QDs clusters. (b) The selected electron diffraction pattern of (a). (c) HAADF-TEM image of spherical superparticles structure. (d) The selected electron diffraction pattern of (c).

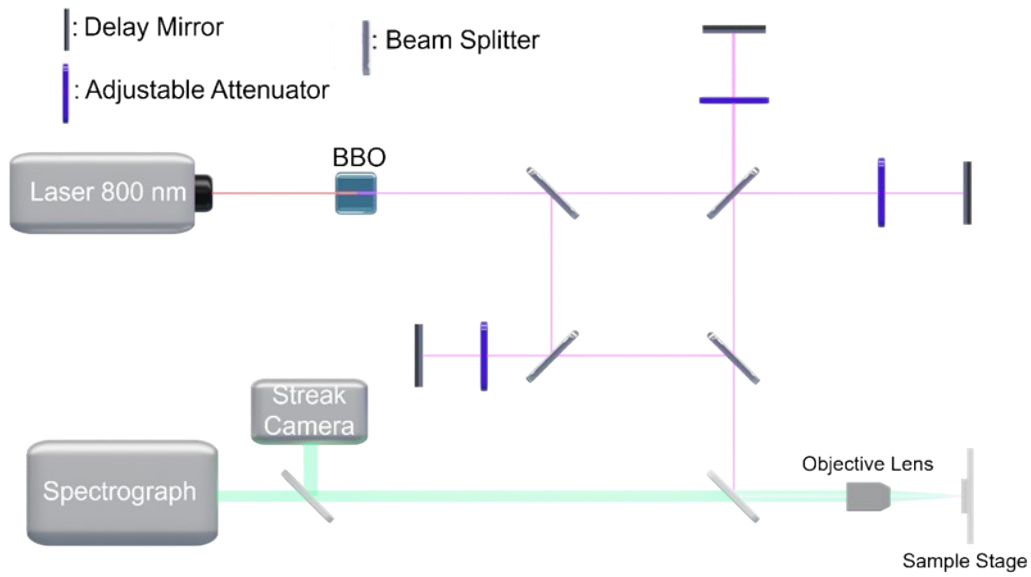


Fig. S8 Schematic diagram of the confocal microscopy photoluminescence system.

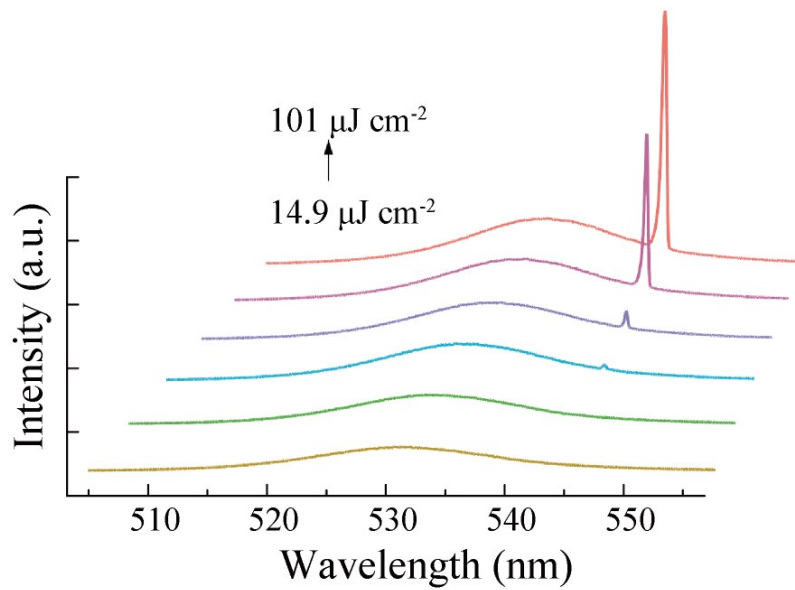


Fig. S9 Typical Excitation power-dependent PL spectra of assembled structures of 6-QDs at 77 K. Pump power density variations from 14.9 to 101 $\mu\text{J cm}^{-2}$.

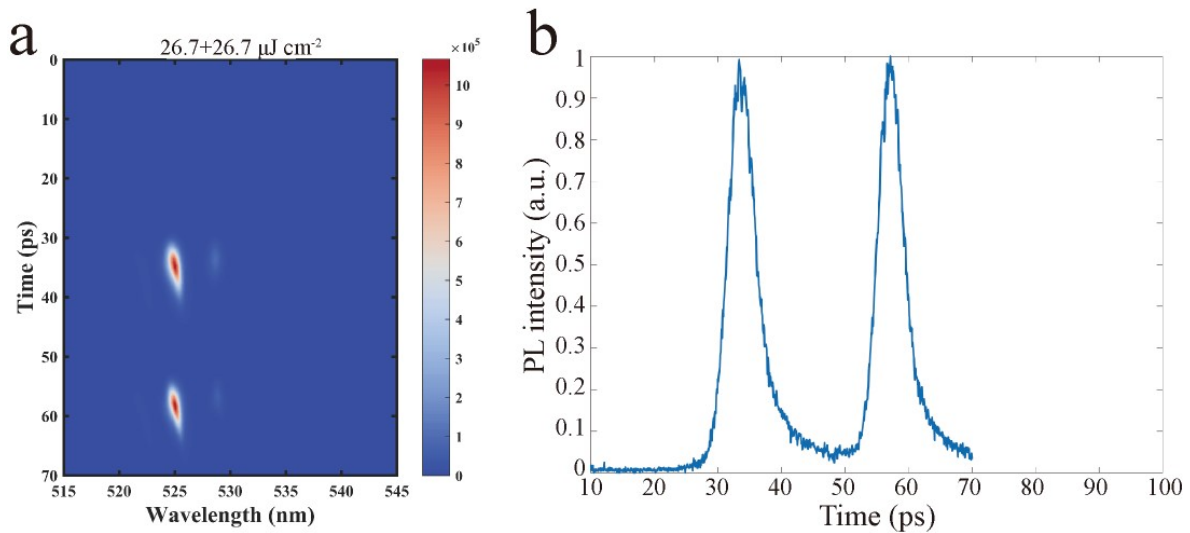


Fig. S10 Surplus dipoles after the CESF process. (a) Streak-camera images of CESF based on 12-QDs spherical superparticles pumping by two laser pulses. (b) Time dynamic CESF spectra of (a) at 525 nm. The spherical superparticles was excited with two femtosecond laser beams in a certain time interval, we chose a laser with an intensity of 1.5 Pth as a reference value, and then the intensity of the excitation light was adjusted. For CESF, in order to make the intensity of the two radiations the same, the energy of the second excitation had to be similar to that of the first. This indicates that after the end of cavity-enhanced superfluorescence, the energy of the inner-medium exciton is consumed.

Table

Table S1. Summary of physical parameters from fitting the spectral vs. temperature variation curve

Intensity				
	A	E_b	E_o	
12-QDs	16.99	70.83	2.454	
6-QDs	38.77	82.96	2.46	
Peak				
	E_o	A_T	A_{EP}	$\hbar\omega$
12-QDs	2.454	0.1674	118.7	135.6
6-QDs	2.46	0.2343	128.8	108.5
FWHM				
	Γ_{inh}	Γ_{AC}	Γ_{LO}	E_{LO}
12-QDs	35.94	30.8	149.1	75.47
6-QDs	37.65	47.3	183.7	76.85

Table S2. Comparison of reported CESF thresholds.

Material	Resonator	Pump source	Threshold	Ref.
InGaAs/GaAs	DBR microcavity	300 fs, 80 MHz	800 $\mu\text{J cm}^{-2}$	1
CsPbBr ₃	WGM microcavity	400 fs, 10 kHz	40 $\mu\text{J cm}^{-2}$	2
CsPbBrCl ₂	WGM microcavity	400 fs, 10 kHz	30 $\mu\text{J cm}^{-2}$	3
CsPbBr ₃	WGM microcavity	400 fs, 10 kHz	15 $\mu\text{J cm}^{-2}$	This work

Table S3. Summary of fitting parameters for PL decay curve

Excitation density	τ_1 (ps)	$A_1/(A_1+A_2)$ (%)	τ_2 (ps)	$A_2/(A_1+A_2)$ (%)
0.3Pth	78.5	100%	-	-
1.1Pth	60.8	63.9	12.94	36.1
1.8Pth	6.634	70.8	50.09	29.2

Supplementary Note 1

Theoretical Model: Dicke Model in a cavity

Based on the *Dicke* model, we study the radiation of cooperative excitons in our samples^{4,5}. Here, the excitons in QDs are simplified as the ideal dipoles in a two level system. The inhomogeneous broadening of QDs is ignored. For the free Hamiltonian of a two-level dipole we have,

$$\hat{H}_1 = \begin{pmatrix} \frac{1}{2}\hbar\omega_0 & 0 \\ 0 & -\frac{1}{2}\hbar\omega_0 \end{pmatrix} \quad (1)$$

where the zero energy has been chosen at the mid-point of the energy interval . The dipole moment operator \hat{d} can be written as an off-diagonal matrix,

$$\hat{d} = \begin{pmatrix} 0 & d_{eg} \\ d_{ge} & 0 \end{pmatrix} \quad (2)$$

All the two-level Hermitian operators can be expressed in terms of the Pauli matrices and the unit 2×2 matrix,

$$\hat{\sigma}_1 = \begin{pmatrix} 0 & 1 \\ 1 & 0 \end{pmatrix} \hat{\sigma}_2 = \begin{pmatrix} 0 & -i \\ i & 0 \end{pmatrix} \hat{\sigma}_3 = \begin{pmatrix} 1 & 0 \\ 0 & -1 \end{pmatrix} \hat{\sigma}_0 = \begin{pmatrix} 1 & 0 \\ 0 & 1 \end{pmatrix} \quad (3)$$

In particular, in accordance with (1) and (2)

$$\hat{H}_1 = \frac{1}{2}\hbar\omega_0 \hat{\sigma}_3 \hat{d} = \text{Re} d \hat{\sigma}_1 + \text{Im} d \hat{\sigma}_2 \quad (4)$$

where $\text{Re} d$ and $\text{Im} d$ are the corresponding real and imaginary parts of d_{ge} .

Let us introduce the quasi-spin operators for the i th dipole

$$\hat{R}_1^{(i)} = \frac{1}{2} \hat{\sigma}_1^{(i)} \quad \hat{R}_2^{(i)} = \frac{1}{2} \hat{\sigma}_2^{(i)} \quad \hat{R}_3^{(i)} = \frac{1}{2} \hat{\sigma}_3^{(i)} \quad (5)$$

and the total quasi-spin operators of the N -dipole system

$$\alpha = 1,2,3 \quad \hat{R}_\alpha = \sum_{i=1}^N \hat{R}_\alpha^{(i)} \quad (6)$$

which obey the usual commutation rules of angular momentum operators

$$\left[\hat{R}_\alpha^{(k)}, \hat{R}_\beta^{(j)} \right] = i\delta_{kj} \hat{R}_\gamma^{(k)} \quad \left[\hat{R}_\alpha, \hat{R}_\beta \right] = i \hat{R}_\gamma \quad (7)$$

Where α, β, γ is any cyclic permutation of the numbers 1,2,3. Then the energy operator of an ensemble of N free identical two-level dipoles can be expressed in the form

$$\hat{H}_N = \sum_{i=1}^N \mathbf{h}\omega_0 \hat{R}_3^{(i)} = \mathbf{h}\omega_0 \hat{R}_3 \quad (8)$$

And its eigenvalues are equal to $\mathbf{h}\omega_0 M$, where $M = \frac{1}{2}N, \frac{1}{2}N-1, \dots, -\frac{1}{2}N$ is the eigenvalue of \hat{R}_3 .

The Hamiltonian for the interaction of such an N -dipole system with the electromagnetic field can be chosen to be in the form

$$\hat{H}_{\text{int}} = -\varepsilon \sum_{i=1}^N \hat{d}^{(i)} = -\varepsilon d \sum_{i=1}^N \hat{R}_1^{(i)} \quad (9)$$

where ε is the operator of the electric field, $\hat{d}^{(i)}$ is the electric dipole moment operator of the i th dipole, $\hat{d}^{(i)} = 2d \hat{R}_1^{(i)}$.

All dipoles are initially in their excited states. The radiative decay of such an ensemble is a cascade of transitions between the adjacent states with the same eigenvalue of \hat{R}^2 equal to $\frac{1}{2}N(\frac{1}{2}N+1)$

$$\left| \frac{1}{2}N, \frac{1}{2}N \right\rangle \rightarrow \left| \frac{1}{2}N, \frac{1}{2}N-1 \right\rangle \rightarrow \dots \rightarrow \left| \frac{1}{2}N, -\frac{1}{2}N \right\rangle \quad (10)$$

The probability per unit time, $\gamma_{M,M-1}$ for a transition $M \rightarrow M-1$, can be obtained,

$$\gamma_{M,M-1} = \gamma \left(\frac{1}{2}N + M \right) \left(\frac{1}{2}N - M + 1 \right) \quad (11)$$

For the SL samples without cavity effect:

When the cooperative dipoles are placed into an *optical cavity*, the parameter γ in equation (11) needs to **enlarge by a factor N_p** , i.e., the effective photon number coupling with dipoles, or the amplification factor of optical field density between the cases ‘with cavity’ and ‘without cavity’. And ***we need to add a new equation to describe the dynamics of N_p*** ,

$$\frac{dN_p}{dt} = \bar{I}(t) - N_p / t_c \quad (12)$$

Here, t_c is the photon lifetime of optical cavity. In addition, a filling factor f describes the ratio between the number N of available hosts for cooperative dipoles and the initially excited dipole number N_0 in the system.

We use the following parameters to obtain the numerical solutions, the excited dipole number by pumping in a cooperative volume $N_0 \in [0 \sim 50]$, the filling factor $f = 3$, the

spontaneous radiative rate $\gamma = 0.0032 \text{ ps}^{-1}$, the cavity photon lifetime $t_c = 7 \text{ ps}$ for the SL sample. The theoretical results are plotted in **Fig. 4e,4f**.

References

- 1 Q. Jie, K. Zhang, C.-W. Lai, F.-K. Hsu, W. Zhang, S. Luo, Y.-S. Lee, S.-D. Lin, Z. Chen and W. Xie, *Physical Review Letters*, 2020, **124**, 157402.
- 2 C. Zhou, Y. Zhong, H. Dong, W. Zheng, J. Tan, Q. Jie, A. Pan, L. Zhang and W. Xie, *Nature Communications*, 2020, **11**, 329.
- 3 L. Chen, D. Mao, Y. Hu, H. Dong, Y. Zhong, W. Xie, N. Mou, X. Li and L. Zhang, *Advanced Science*, 2023, **10**, 2301589.
- 4 R. H. Dicke, *Physical Review*, 1954, **93**, 99-110.
- 5 M. G. Benedict, A. M. Ermolaev, V. A. Malyshev, I. V. Sokolov, E. D. Trifonov, *Super-radiance: Multiatomic Coherent Emission*, Institute of Physics Publishing, London 1996.